

S. M. Frolov · V. Ya. Basevich · V. S. Aksenov ·  
S. A. Polikhov

## Optimization study of spray detonation initiation by electric discharges

Received: 14 November 2003 / Accepted: 15 December 2004 / Published online: 12 September 2005  
© Springer-Verlag 2005

**Abstract** Development of air-breathing pulse detonation engines is faced with a challenging problem of detonation initiation in fuel sprays at distances feasible for propulsion applications. Extensive experimental study on initiation of a confined *n*-hexane spray detonation in air by electric discharges is reported. It is found that for direct initiation of spray detonation with minimal energy requirements (1) it is worth to use one discharger located near the closed end of a detonation tube and at least one additional discharger downstream from it to be triggered in-phase with primary shock wave arrival; (2) the discharge area should be properly insulated to avoid electric loss to metal tube walls; (3) discharge duration should be minimized to at least 50  $\mu$ s; (4) discharge channel should preferably occupy a large portion of a tube cross-section; (5) test tube should be preferably of a diameter close to the limiting tube diameter; (6) gradual transition between the volume with electric discharger and the tube should be used; and (7) a powerful electric discharger utilized for generating a primary shock wave can be replaced by a primary shock wave generator comprising a relatively low-energy electric discharger, Shchelkin spiral, and tube coil. With all these principles implemented, the rated electric energy of about 100 J was required to initiate *n*-hexane spray-air detonation in a 28-mm tube at a distance of about 1 m from the atomizer.

**Keywords** Detonation initiation · Liquid-fuel spray · Electric discharge · Pulse detonation engine

**PACS** 02.60.Cb; 05.10.Ln; 47.11.+j; 47.15.Cb; 47.40.Nm

This paper was based on work that was presented at the 19th International Colloquium on the Dynamics of Explosions and Reactive Systems, Hakone, Japan, July 27 - August 1, 2003

Communicated by J.E. Shepherd

S. M. Frolov (✉) · V. Ya. Basevich  
Russian Academy of Sciences, N.N. Semenov Institute of Chemical Physics, Department of Combustion and Explosion, 4 Kosigin Street, Moscow 119991, Russia  
E-mail: smfrol@chph.ras.ru

V. S. Aksenov · S. A. Polikhov  
Moscow Physical Engineering Institute (Technical University),  
31 Kashirskoe Shosse, Moscow 115522, Russia

### Nomenclature

$C$	capacitance
$E$	rated electric energy of a discharge
$E_{\min}$	critical energy of detonation initiation
$E_p$	primary discharge energy
$J$	electric current
$L$	length
$l$	length
$S$	tube cross-section
$U_{\min}$	minimal capacitor voltage required for detonation initiation
$U$	voltage
$V$	shock wave or reaction front velocity
$X$	distance between measuring stations
$\Delta C$	uncertainty in determining the capacitance $C$
$\Delta E$	uncertainty in determining the rated electric energy $E$
$\Delta t$	time interval
$\Delta t_d$	delay time of triggering the second discharger
$\Delta U$	uncertainty in determining the voltage $U$
$\Delta V$	uncertainty in determining the velocity $V$

### Indices

1	related to the first discharger
2	related to the second discharger

### 1 Introduction

One of challenging problems encountered in the development of an air-breathing pulse detonation engine is detonation initiation in fuel sprays at distances feasible for propulsion applications. In view of it, there is a need in experimental data on detonation initiation and propagation in heterogeneous fuel-air mixtures under well-defined conditions. The latter applies to the initiation means, initiator location, energy deposition history, geometry and physical properties of confinement, homogeneity and properties of fuel-air mixture, etc.

For direct initiation of gaseous detonations these issues were addressed, for example, by Matsui and Lee [1], and reviewed by Nettleton [2] and Roy et al. [3]. Fuel spray–air detonations are usually initiated by high-explosive charges [4], shock waves [5], or fuel–oxygen detonations [6]. This paper addresses some of the issues listed earlier and shows possibilities to minimize energy requirements for direct initiation of spray detonation by electric discharges.

## 2 Basic setup

The basic test facility is a steel tube 51 mm in diameter and 1.5 m long. To create a two-phase flow, an air-assist atomizer is mounted at one end of the tube. The atomizer is attached to the tube via the expanding conical transition section. The other end of the tube is connected to the atmosphere via a detonation arrester consisting of a cylinder packed with metallic strips. Air supply system comprises a compressor, bottle, and air solenoid valve. Liquid fuel supply system consists of a pressurized fuel tank and a fuel solenoid valve. The air bottle and fuel tank are pressurized to preset pressure values before each run, usually to  $6.00 \pm 0.05$  and  $5.3 \pm 0.05$  atm, respectively. These values were found in a series of experiments aimed at establishing the optimal fuel-supply pressure at a given air pressure. This optimal fuel pressure resulted in the maximal visible flame propagation velocity in the basic setup. When the solenoid valves are activated, air and fuel are directed to the atomizer that provides the entire mixture flow rate through the tube. Pulse flow duration in the reported experiments is about 1 s. The liquid fuel used is *n*-hexane. The initial temperature of air and liquid fuel was  $293 \pm 4$  K. At the beginning of the experiments, the tube temperature was  $293 \pm 4$  K.

Ignition of two-phase flow is facilitated by a powerful electric discharger with a capacitor fed with a high-voltage rectifier. The discharger has a three-electrode scheme and consists of primary (breakdown) and main discharge gaps (Fig. 1a) 3- and 8-mm size, respectively. Diameter of copper electrodes is 2.5 mm. They protrude from the tube wall by 14 mm and are bended a little along the flow direction.

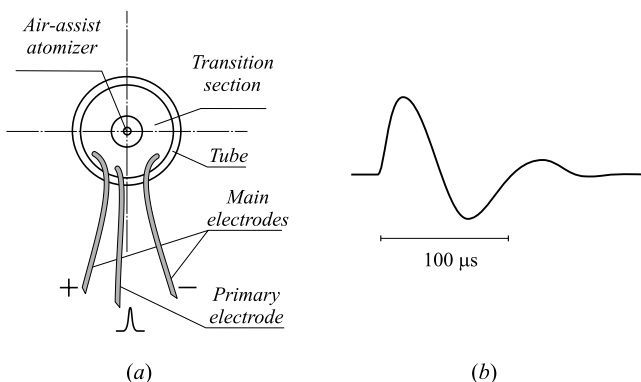


**Fig. 1** **a** Schematic of a three-electrode electric discharger; and **b** typical shape of the discharge current

The initiating primary electrode is positioned upstream from the main electrodes. The casing of the discharger is made of steel and has a thread to be fixed in the port of the detonation tube. The cylindrical insulator 20 mm in diameter is made from Teflon and is fixed in the casing with the composite containing glass fiber and epoxy compound. The electric connections are made of the copper wire of  $2 \times 2.5$  mm cross-section and 300 mm long. The rated energy,  $E$ , deposited by the discharger is calculated based on the primary discharge energy  $E_p$ , capacitance  $C$ , and voltage  $U$ , that is  $E = E_p + CU^2/2$ . The primary discharge is of fixed ( $E_p = 57$  J) energy. Capacitance of the main discharge is  $600 \mu\text{F}$ . The maximal voltage is 3,500 V. The uncertainty in the  $C$  value is less than 1%. The total error in determining the capacitor voltage is estimated as less than 1%. The uncertainty in determining the energy  $E$ , calculated as  $\Delta E/E = \Delta C/C + 2\Delta U/U$ , does not exceed 3% at a voltage of 2,000 V. After a discharge, the residual voltage of the capacitor does not exceed 400 V. Taking into account the residual energy in the capacitor, the maximal error in determining the  $E$  value at  $U = 2,000$  V does not exceed 7%. Note that the actual energy transferred to the combustible mixture is considerably less than the rated energy of the electric discharge. According to Nettleton [2], it can amount only 10% of the rated energy and depend on various factors. For the basic setup, the measurements of the discharge current and voltage indicate that the discharge efficiency is about 20–25%. Nevertheless, in the study reported herein the minimal rated energy  $E$  for spray detonation initiation is used as a criterion for setup optimization, as this parameter is readily determined. The issues dealing with quantitative estimation of the discharge efficiency are out of the scope of this paper.

The discharger is located inside a conical transition section at a distance of 60 mm downstream from the atomizer nozzle. The characteristic time of discharge is  $100 \mu\text{s}$  (Fig. 1b). A digital controller controls opening and closing of the air and fuel solenoid valves and discharge triggering.

Several air-assist atomizers were designed, fabricated, and tested. Schematic of the atomizer used in the basic setup is shown in Fig. 2. Air is supplied via two radial channels 2.6 mm in diameter and 7 mm long. Liquid fuel is supplied via one 0.28-mm diameter and 1 mm long axial channel into one of the air channels. The diameter of the atomizer nozzle is 3 mm. This atomizer provides the flow rate of air of about 20 g/s.

Intense mixing of liquid fuel with air in the atomizer nozzle results in a spray with very fine fuel drops. For measuring drop size distribution, the slide sampling method reported by Elkotb [7] was used. In this method, a slide with thinly coated soot deposited from a candle flame is introduced into the fuel spray for a short time. The footprints left by the impinging droplets in the soot are then photographed under the microscope. Figure 3 shows drop size distribution at a distance of 100 mm downstream from the nozzle. The arithmetic mean diameter of drops at this distance from the atomizer nozzle is close to  $5\text{--}6 \mu\text{m}$ . Figure 4 shows a photograph

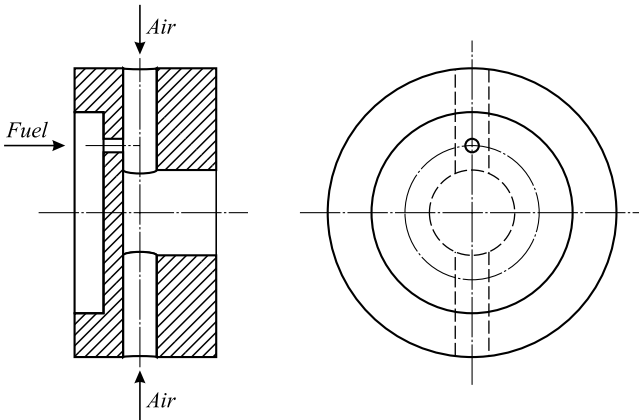


**Fig. 2** Schematic of the air-assist atomizer used in the basic setup

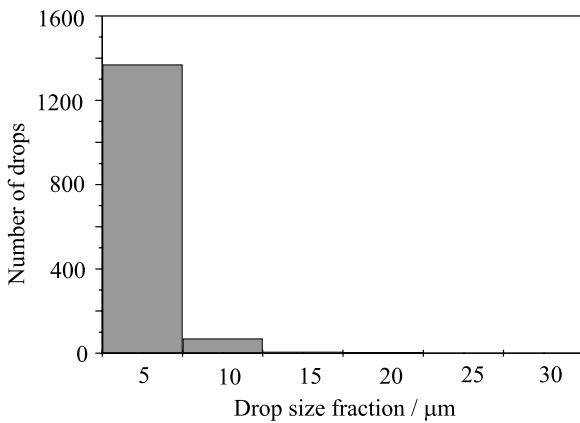


**Fig. 3** Drop size distribution 100 mm downstream from the atomizer nozzle

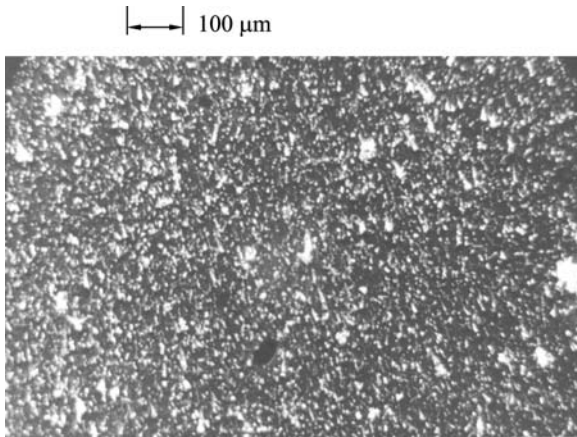


**Fig. 4** Photograph of a liquid spray signature on a target plate at a distance of 70 mm from the atomizer nozzle

of spray signature on a target plate at a position close to the discharge electrodes—70 mm downstream from the atomizer nozzle. In view of the data presented in Figs. 3 and 4 the discharge is located in the two-phase flow region during the experiments. At distances exceeding 300 mm, no drops were detected in the flow virtually due to their complete evaporation. The estimates based on the approach of Frolov et al. [8]

show that drops of initial diameter 10–11  $\mu\text{m}$  should evaporate at distances less than 200 mm under conditions of our experiments and attain the size of 5–6  $\mu\text{m}$  at a distance of 100 mm downstream from the atomizer nozzle. These results correlate with the measurements.

The fuel consumption was determined by measuring fuel level in the tank after several experimental runs at similar initial conditions. Air consumption was calculated based on the pressure difference in the air bottle before and after the runs. The mean equivalence ratio in most of runs was  $1.3 \pm 0.1$ , that is the fuel–air mixture was always fuel rich. This effect is attributed to the partial deposition of the injected fuel on the inner wall of the tube. In fact, measurements without ignition reveal the existence of the liquid fuel film deposited on the inner tube wall up to distances of about 600 mm from the atomizer nozzle.

Measuring stations in the basic setup are located 500, 900, and 1,300 mm downstream from the discharger and comprise a piezoelectric pressure transducer (PT) and ionization probe mounted on the opposite walls. Measuring segment 1 includes the discharger and first measuring station with the characteristic distance of 500 mm. Measuring segments 2 and 3 are 400 mm long each. The velocity of the combustion fronts as well as shock and detonation waves was calculated using the formula  $V = X/\Delta t$ , where  $X$  is the length of the measuring segment and  $\Delta t$  is the time interval determined from the records of the ionization probes and/or PTs. The time interval  $\Delta t$  was determined with the uncertainty of  $\pm 2.4 \mu\text{s}$ . The detonation velocity in the *n*-hexane–air mixture is at the level of 1,700–1,800 m/s. Hence, the maximal error in determining the time interval  $\Delta t$  is  $\pm 1\%$  at the measuring segment 400 mm long, and less than  $\pm 1\%$  at the measuring segment 500 mm long. The error in determining the detonation velocity at these measuring segments does not exceed 1.25%. The shock wave velocities in the experiments are smaller than the detonation velocity. Therefore, the error,  $\Delta V/V$ , of determining the shock wave velocity is smaller than that for the detonation velocity.

### 3 Spray detonation initiation in the basic setup

The aim of the tests described in this section was to determine the critical energy of direct detonation initiation by the electric discharger of Fig. 1. At the voltage of 3,200 V between the main electrodes corresponding to the discharge energy of 3,130 J (including the primary discharge energy), no detonation was observed in the basic setup. Increasing voltage from 3,200 to 3,300 V, which is equivalent to increasing the discharge energy from 3,130 to 3,320 J, resulted in detonation initiation and propagation at all measuring segments. Further increase of the discharge energy from 3,320 to 3,730 J exerted no effect on the detonation parameters. In runs with successful detonation initiation, detonation waves propagated at the mean velocity of  $1,780 \pm 100 \text{ m/s}$  at measuring segments 2 and 3. This value is close to the thermodynamic Chapman–Jouguet detonation velocity

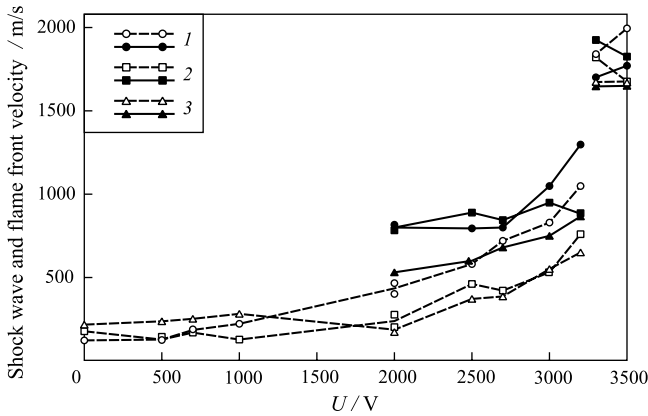


**Fig. 5** Measured shock wave (solid curves) and flame front (dashed curves) velocities vs. voltage at main discharge electrodes. Numbers 1–3 correspond to measuring segments 1–3

in a homogeneous stoichiometric *n*-hexane–air mixture (1,840 m/s). Deviations between the measured detonation velocity and its thermodynamic value can be caused by spatial inhomogeneity of mixture composition and various loss mechanisms pertinent to confined detonations.

Figure 5 summarizes the results of experiments with different voltage at the main electrodes. Dashed and solid curves correspond to measured flame and shock wave velocities, respectively, at the corresponding measuring segments (denoted as 1, 2, and 3). At the voltage equal or exceeding  $U_{\min} = 3,300$  V, the detonation arises at all measuring segments, i.e., at  $E \geq E_{\min} = 3,300$  J, direct detonation initiation is observed. This value will be referred to as the critical energy of direct detonation initiation in the basic setup.

The results of Fig. 5 also indicate that deflagration-to-detonation transition (DDT) does not occur in the basic setup. At a relatively low discharge voltage,  $U < 1,000$  V, the visible flame velocity slightly increases along the tube. However, at a higher discharge voltage, the visible flame velocity always decreases along the tube. A shock wave generated by the discharge also decelerates. Thus, there is no evident indication of flame and shock wave acceleration typical for DDT.

## 4 Optimization study

The aim of the optimization study is to decrease the discharge energy required for direct detonation initiation by improving certain elements of the basic experimental setup.

### 4.1 Discharger location

Positioning of the discharger at a distance of 100 mm downstream from its position in the basic setup results in increasing the critical voltage from  $U_{\min} = 3,300$  to 4,100 V, i.e., increasing the critical initiation energy by more than 50%—from 3,300 to 5,100 J. This result is evidently caused by a

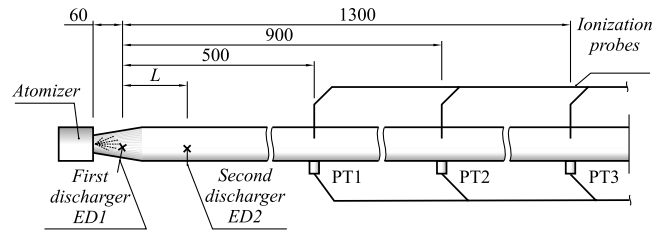


**Fig. 6** Schematic of the detonation tube with two dischargers. PT1, PT2, and PT3 denote pressure transducers. Dimensions are in millimeters

weaker effect of the reflecting end of the tube on the shock wave generated by the discharge.

### 4.2 Successive triggering of two dischargers

Figure 6 shows the sketch of the detonation tube with two electric dischargers. The first discharger, ED1, is the same as that used in the basic setup. It is located 60 mm downstream from the atomizer nozzle. The second discharger, ED2, is mounted at distance  $L$  from the first discharger. Its configuration is similar to that shown in Fig. 1. The aim of the tests described in this subsection was to amplify a decaying primary shock wave generated by the first discharger to a detonation by means of controlled triggering of the second discharger. In this case, the second discharger is used for inducing vigorous explosion of the reactive mixture in the close vicinity to the decaying shock wave and transforming it to a detonation according to the mechanisms discussed by Frolov et al. [9, 10, 11, 12]. Figure 7 shows a typical discharge current in a two-discharge circuit. In this case, the second discharge is triggered with the delay time  $\Delta t_d$ .

The experimental procedure encountered a number of steps dealing with ‘tuning’ the digital controller in terms of the preset triggering delay time  $\Delta t_d$  of the second discharger located at a distance of  $L = 100, 200, 300,$  or 400 mm downstream from the first discharger. The ‘tuning’ was aimed at obtaining a detonation wave at the measuring segment 2 (between PT1 and PT2, see Fig. 6) and 3 (between PT2 and PT3) with the lowest possible total discharge energy  $E = E_1 + E_2$ , where  $E_1$  and  $E_2$  are the energies of the first and the second dischargers, respectively.

The procedure was as follows. Capacitances of the first and the second dischargers were identical (300  $\mu$ F), so their total capacitance was the same as in the tests with one discharger. The ignition energy was controlled by voltage

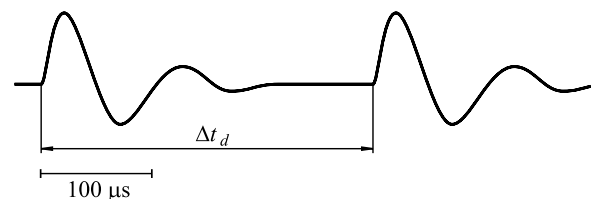


**Fig. 7** Typical record of discharge current in a two-discharge circuit

(identical for both dischargers). The maximum voltage used was  $U = 3,000$  V that is lower than the minimal voltage required for detonation initiation by one discharger (3,300 V). After triggering the first discharger, the primary shock wave arrival time at PT1, PT2, and PT3 was detected and the shock wave velocity at measuring segments between ED1 and PT1 (segment ED1–PT1), between PT1 and PT2 (PT1–PT2), and between PT2 and PT3 (PT2–PT3) was obtained. Based on these data, a first approximation for the triggering delay time of the second discharger was obtained for the next run. This time delay was preset in the controller. The next run encountered time-delayed triggering of both dischargers. Shock wave velocity at segments PT1–PT2 and PT2–PT3 was then measured at this preset value of the triggering delay time  $\Delta t_d$ . In the subsequent runs, the delay time was varied in a certain vicinity of this value to reveal the best conditions for shock wave amplification to a detonation. Then voltage  $U$  was decreased and a new test series at a lower total discharge energy was performed. At each stage of the procedure, several runs were performed to collect statistics on reproducibility of results. It has been found that the results were satisfactorily reproducible.

Figure 8 summarizes the results of experiments for  $L = 200$  mm in the form of the  $U$  versus  $\Delta t_d$  plot. Plus and minus signs correspond to reliable “go” and “no go” detonation conditions at segments PT1–PT2 and PT2–PT3. There exist resonant conditions for second discharger triggering in terms of the delay time  $\Delta t_d$ . The “width” of the detonation peninsula is about  $50 \mu\text{s}$  at 3,000 V and  $10 \mu\text{s}$  at 2,500 V. At a fixed delay time, e.g.,  $\Delta t_d = 270 \mu\text{s}$ , the detonation arises at 2,500 V and does not arise at a higher voltage (2,600–2,900 V). This indicates the necessity of careful synchro-

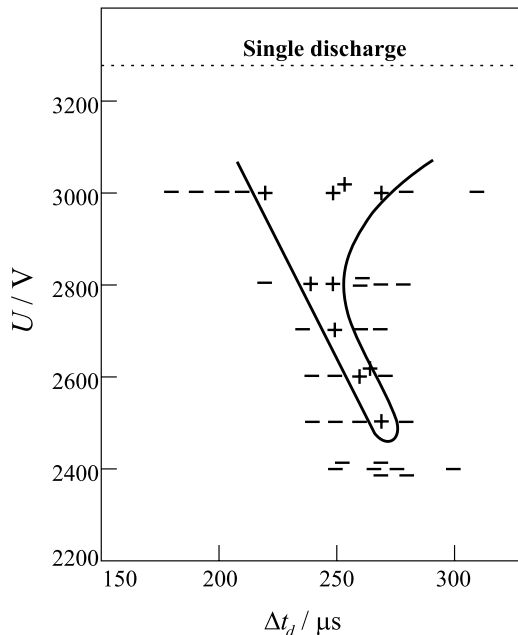


**Fig. 8** Results of experiments on detonation initiation by two successively triggered dischargers mounted 200 mm from each other

**Table 1** Critical voltage  $U_{\min}$ , critical total discharge energy  $E_{\min}$ , and optimal delay time  $\Delta t_d$  required for detonation initiation with two successively triggered dischargers depending on distance  $L$  between them

$L$ (mm)	$U_{\min}$ (V)	$E_{\min}$ (kJ)	$\Delta t_d$ ( $\mu\text{s}$ )
100	3,000	2.800	100
200	2,500	2.000	270
300	3,000	2.800	380
400	>3,000*	>2.800	430

\*At  $U = 3,000$  V, the highest detected shock wave velocity at measuring segment PT2–PT3 was 1,400 m/s

nization of second discharger triggering with the arrival of the shock wave generated by the first discharger. The lowest voltage required for detonation initiation with two successively triggered dischargers is  $U_{\min} = 2,500$  V instead of 3,300 V relevant to the tests with one discharger (dotted line in Fig. 8). This decrease in voltage indicates almost two-fold decrease in the total critical detonation initiation energy. It is worth noting that the capability of the second discharger to initiate detonation is considerably lower than that of the first discharger, as discussed in Sect. 4.1.

Table 1 shows the critical values of voltage,  $U_{\min}$ , the total discharge energy,  $E_{\min}$ , and the optimal delay time  $\Delta t_d$  required for detonation initiation with two successively triggered dischargers depending on  $L$ . The optimal distance between the dischargers is about 200 mm. At this distance, the critical detonation initiation energy attains a minimal value.

#### 4.3 Discharge parameters

To improve the efficiency of the electric discharge in terms of energy transition to the test mixture, the following measures were used: (1) interior surface of the diverging transition section connecting the atomizer and the tube was covered with a 1-mm thick layer of dielectric thermo-resistant lacquer. This avoided a discharge between the main electrodes and metal walls of the transition section; (2) electric connection between the electrodes and the capacitors was made using a coaxial cable, rather than separate wires. These and some other minor modifications led to transformation of the discharge current shape and decrease in the effective discharge duration from 100 to  $50 \mu\text{s}$  (Fig. 9). With the modified discharger, the critical voltage required for direct detonation initiation by a single discharge decreased from  $U_{\min} = 3,300$  to 2,200 V, resulting in the decrease of the critical initiation energy from 3,320 to 1,510 J, i.e., more than by a factor of 2.

#### 4.4 Optimization of atomizer

To increase the airflow rates in the detonation tube and therefore to increase the level of turbulence, the atomizer of Fig. 2 was modified as shown in Fig. 10. The modified atomizer has six air-supply radial channels 2.6 mm in diameter and

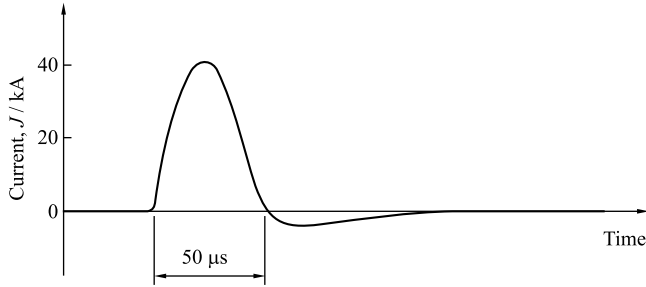


**Fig. 9** Shape of discharge current after discharger modification

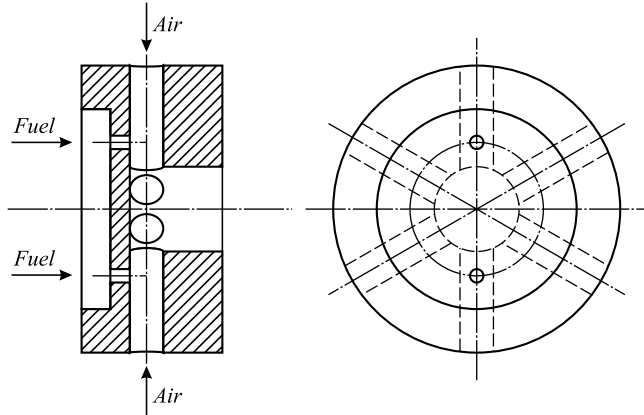


**Fig. 10** Schematic of the modified air-assist atomizer

7 mm long and two fuel-supply axial channels 0.26 mm in diameter and 1 mm long. The diameter of the atomizer nozzle is 6 mm. The airflow rate of the modified atomizer is about 30 g/s. This atomizer produces a higher level of turbulence in the flow as compared to the atomizer of Fig. 2, while providing an approximately similar drop size distribution. With the new atomizer and a single modified discharger, a detonation was initiated at  $U_{\min} = 2,100$  V, i.e., there was no considerable difference in the performances of the atomizers of Figs. 2 and 10.

#### 4.5 Optimization of detonation tube

To study the effect of tube diameter on the critical detonation initiation energy, several modifications of the experimental setup were made. Figure 11a–c shows the setups with a 28-mm-diameter detonation tube. In the setups of Fig. 11a and b, the assembly with a diverging transition section is the same as in the basic setup. In the setup of Fig. 11a, two possibilities are foreseen to connect the transition section with the detonation tube: either immediately through the converging section 65 mm long, or through a cylindrical section of length  $l$ , followed by a converging section. Figure 12 shows the results of experiments with one discharger and  $l = 0$ . Contrary to Fig. 5, the dependency of the shock wave velocity on the discharge voltage is smooth. There is no evident abrupt change in the mode of shock wave propagation after attaining the velocity of 1,200 m/s. In runs with the voltage

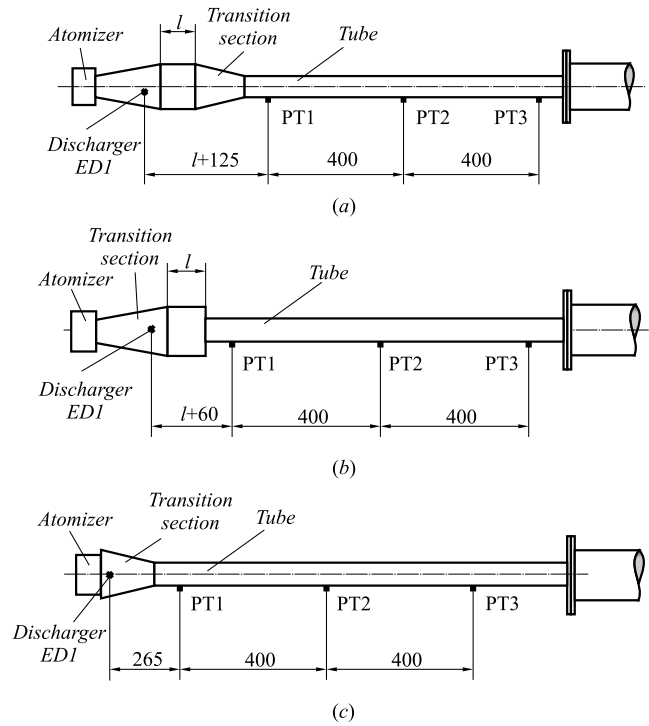


**Fig. 11** Modified experimental facilities with a 28-mm detonation tube. **a** Setup with the diverging–converging transition section. **b** Setup with the diverging section and abrupt transition to the detonation tube. **c** Setup with the converging transition section. PT1, PT2, and PT3 denote pressure transducers. Dimensions are in millimeters

equal or exceeding  $U_{\min} = 1,600$  V, successful detonation initiation was detected at measuring segments PT1–PT2 and PT2–PT3. The mean detected detonation velocity in several runs is  $1,700 \pm 50$  m/s. A regular variation of the lead shock wave velocity with the discharge voltage may be explained

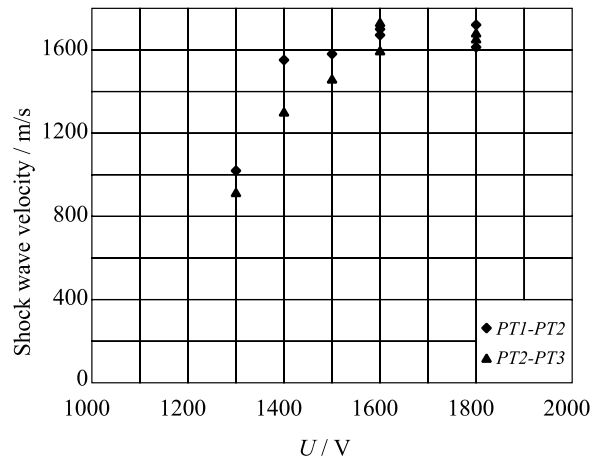


**Fig. 12** Measured shock wave velocities vs. discharge voltage. Measuring segments PT1–PT2 and PT2–PT3 correspond to the detonation tube of Fig. 11a with no cylindrical insert ( $l = 0$ ); atomizer of Fig. 10 and discharge shape of Fig. 9

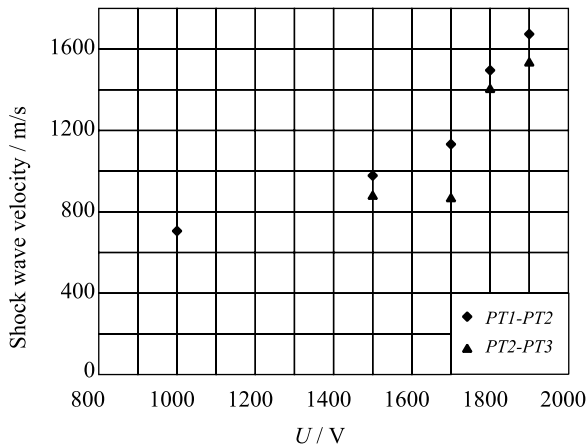


**Fig. 13** Measured shock wave velocities vs. discharge voltage. Measuring segments PT1–PT2 and PT2–PT3 correspond to the detonation tube of Fig. 11a with a cylindrical insert ( $l = 90$  mm), atomizer of Fig. 10 and discharge shape of Fig. 9

by the proximity of the tube diameter (28 mm) to the limiting tube diameter for the  $n$ -hexane–air mixture.

The voltage of 1,600 V corresponds to a critical initiation energy of about  $E_{\min} = 820$  J, which is by a factor of 4 less than in the basic setup. Note that with decreasing the main discharge capacitance from 600 to 400  $\mu$ F, the minimal voltage of about 1,900 V was required to initiate a detonation in the setup of Fig. 11a with  $l = 0$ . This voltage corresponds to the critical initiation energy of about 780 J, which is close to that found in tests with a higher discharge capacitance (820 J). The difference is probably explained by different residual energies stored by the capacitors after discharge.

A cylindrical insert in the setup of Fig. 11a does not improve the detonation initiation conditions. Figure 13 shows the results of experiments at  $l = 90$  mm. In this case, the critical discharge voltage required for detonation initiation is 1,900 V, which corresponds to the initiation energy of 1,140 J. This energy is 40% higher than that obtained in the setup of Fig. 11a without cylindrical insert.

Replacement of the converging section with an abrupt transition to the detonation tube as in the setup of Fig. 11b also deteriorates the detonation initiation conditions. For example, at  $l = 50$  mm, the minimal voltage required for detonation initiation in the setup of Fig. 11b increases to 2,100 V ( $E_{\min} = 1,380$  J).

In the setup of Fig. 11c, the other type of discharge – sliding discharge – has been used. Figure 14 shows a schematic of the unit with the sliding discharge. Casing 1 is made of dielectric polycarbonate glass. Electrodes 2 and 4 are used for the main discharge, while electrode 3 serves for discharge initiation. Five carbon-graphite bars 5 of 2  $\times$  4 mm cross-section are fixed in the casing. Specific resistance of the bar material is 2.5  $\Omega$ /mm. Fluoroplastic washers 0.2-mm thick are laid between bar edges to create four discharge gaps 7. The axial opening in the casing is used for delivery of the fuel–air mixture from the atomizer. The gap be-

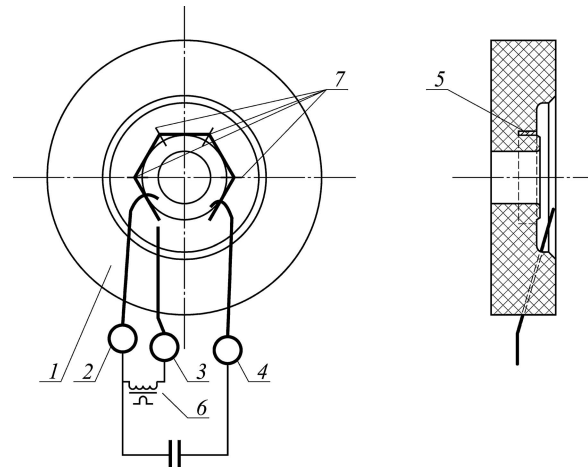


**Fig. 14** Sliding discharge configuration. 1: casing; 2, 3, and 4: electrodes; 5: carbon-graphite bars; 6: pulse transformer; and 7: discharge gaps

tween main electrode 2 and the closest carbon-graphite bar is large. Therefore, when pulse transformer 6 receives the initiating signal, breakdown occurs between electrodes 3 and 4 via all gaps 7. Then, starting from each gap 7, plasma leaders form and propagate along the bar surface. Plasma leaders close-circuit the bars and electric current increases. The arc current is limited by the resistance of the bars and does not exceed 20 A. The main breakdown between electrodes 2 and 4 occurs after joining of all plasma leaders. The main discharge current attains 10 kA. Discharge channel is a curve of about 50-mm length and mean diameter of about 23 mm.

In the experiments with the discharge of Fig. 14, the discharge capacitance was 300  $\mu$ F. Voltage was varied from 2,000 to 2,200 V. The delay time of the main discharge breakdown was affected by the speed of the plasma leaders. After several discharges (“training”), the average delay time was about 200  $\mu$ s. Nevertheless, deviations of the actual triggering time from the average value attained 100  $\mu$ s. The results of experiments are summarized in Fig. 15. Increasing the voltage from 2,000 to 2,100 V (from 600 to 660 J in terms of energy) resulted in direct detonation initiation in the tube. The mean detonation velocity was  $1,700 \pm 50$  m/s at all three measuring segments, namely, at the segments ED1–PT1, PT1–PT2, and PT2–PT3 (see Fig. 11c). Increase of the discharge energy to 730 J did not change the mean detonation velocity.

The use of the sliding discharge instead of the arc discharge resulted in the decrease of the critical energy of detonation initiation in the 28-mm tube from about 820 to about 660 J. Figure 16 shows the corresponding sample pressure records at different initiation energies. The control channel in Fig. 16 shows the record of a discharge circuit with discharge timing and shape. At  $U = 2,000$  V detonation initiation fails, while at  $U = 2,100$  and 2,200 V detonation is detected.

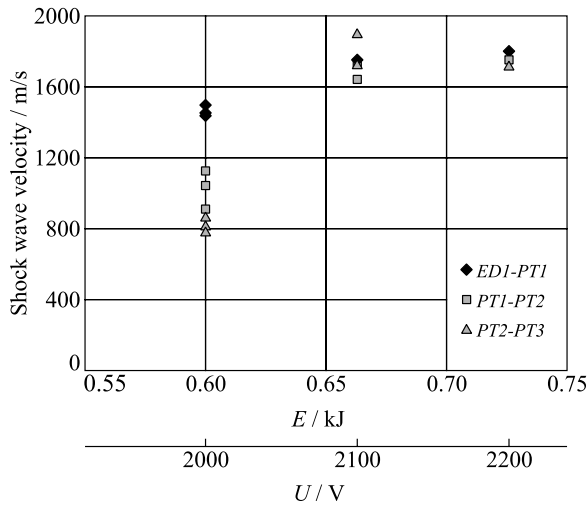


**Fig. 15** Measured shock wave velocities vs. discharge energy and voltage in tests with the sliding discharge of Fig. 14. Measuring segments ED1–PT1, PT1–PT2, and PT2–PT3 correspond to the detonation tube of Fig. 11c

#### 4.6 Combined modifications

The experimental setup of Fig. 17 combines several modifications of the basic setup described so far. It comprises a 28-mm diameter detonation tube in the configuration of Fig. 11c, the atomizer of Fig. 10, and two arc dischargers with the current shape similar to that shown in Fig. 9. In this setup, the first discharger was mounted very close to the atomizer nozzle. The distance between the first and the second dischargers was 200 mm. The capacitance of each discharger was 200  $\mu\text{F}$ , and the discharge voltage was 2,000 V. Under these conditions, the energy stored by the capacitors of each discharger is  $E_1 = E_2 = 460 \text{ J}$  and the total energy is  $E = 920 \text{ J}$ .

Figure 18 shows the dependence of the shock wave velocity on the triggering delay time  $\Delta t_d$  of the second discharger. A detonation was successfully initiated only at some values of  $\Delta t_d$ . The detonation peninsula is very narrow: detonation was detected at  $\Delta t_d$  ranging from 212 to 215  $\mu\text{s}$ . Figure 19a and 19b shows the samples of pressure records with successful detonation initiation ( $\Delta t_d = 214 \mu\text{s}$ , Fig. 19a) and initiation failure ( $\Delta t_d = 211 \mu\text{s}$ , Fig. 19b). When the discharger of Fig. 14 was used as the first discharger, it was difficult to “tune” the time delay  $\Delta t_d$  to hit in the narrow detonation peninsula of Fig. 18. Therefore, the configuration with the sliding discharge was treated as impractical.

To further decrease the initiation energy, a powerful electric discharger utilized for generating a primary shock wave was replaced by a primary shock wave generator comprising a relatively low-energy electric discharger and a Shchelkin spiral (Fig. 20). This decision was made based on the analysis of Fig. 5. In the basic experimental setup, the air-assist atomizer used for spraying liquid *n*-hexane in air provides a highly turbulent two-phase reactive flow in the tube. Ignition of the flow with a powerful discharge results in the

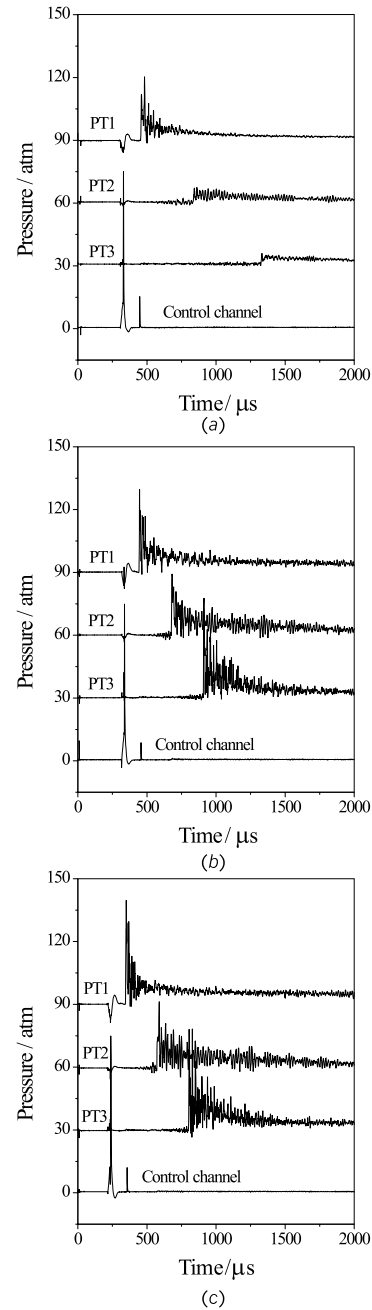


**Fig. 16** Sample pressure records obtained in the setup of Fig. 11c with the sliding discharge of Fig. 14 at a voltage of **a** 2,000 V (energy 600 J), **b** 2,100 V (660 J), and **c** 2,200 V (730 J). Records PT1, PT2, and PT3 correspond to pressure transducers in Fig. 11c. Control channel shows a record of the discharge circuit. The mean detonation velocity is  $1,713 \pm 21 \text{ m/s}$  **b** and  $1,735 \pm 21 \text{ m/s}$  **c**

generation of a primary shock wave followed by the turbulent flame. The experimental results obtained for detonation initiation in a 51-mm diameter tube with one discharge indicate that the propagation velocities of both the lead shock wave and flame front are nearly independent of the discharge energy once the latter is less than about 50% of the critical initiation energy of detonation (see Fig. 5). This implies

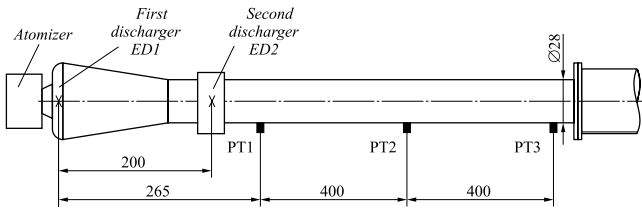


**Fig. 17** Schematic of the detonation tube with the converging transition section and two dischargers. PT1, PT2, and PT3 stand for pressure transducers. Dimensions are in millimeters

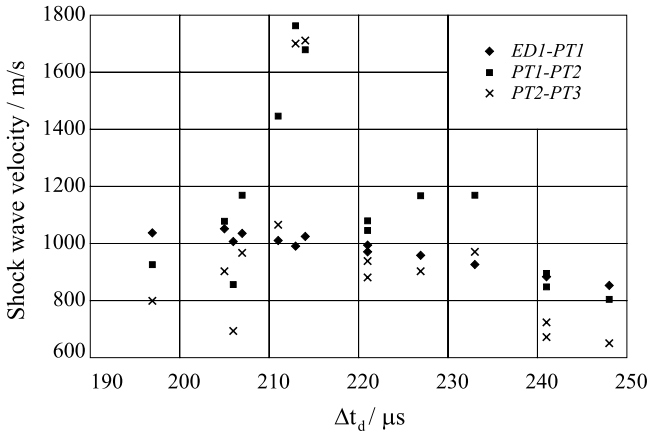


**Fig. 18** Dependence of the shock wave velocity on the triggering delay time of the second discharger in the setup of Fig. 17. Measuring segments ED1–PT1, PT1–PT2, and PT2–PT3 correspond to the setup of Fig. 17

that the turbulence generated by the air-assist atomizer could play an important role in the primary shock generation at the discharge energies less than about a half of the critical energy. At higher discharge energies, flame propagation is increasingly affected by the discharge-generated shock wave. In view of it, enhancement of turbulence produced by the atomizer could potentially be used for decreasing the discharge energy required for a powerful primary shock wave to form.

The experimental setup of Fig. 20 was comprised of a 28-mm diameter tube with the Shchelkin spiral 460 mm long and two electric dischargers ED1 and ED2. The spiral was made of steel wire 4 mm in diameter and had an 18-mm pitch. As in the setup of Fig. 20 the shock wave arrival time to the second discharger varied within the wide range—from 1,400 to 2,000  $\mu s$ —a special discharge activation probe was used to provide the precise synchronization of the second discharger triggering time with the primary shock wave arrival. The probe was made of tungsten wire 0.8 mm in diameter and had a form of a rectangular frame 6 × 10 mm size positioned at the tube axis. The probe triggered the time-delay circuit in the digital controller, which, in its turn, triggered the second discharger. The probe was mounted at a distance of 90 mm upstream from the position of the second discharger. Electric conductivity of the medium behind the propagating shock wave was sufficient for activating the probe with the saturation current of about 1 mA.

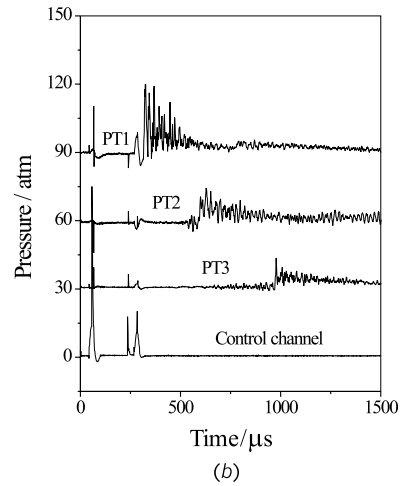
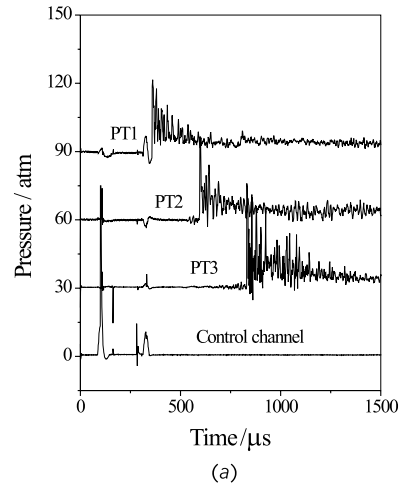


**Fig. 19** Sample pressure records with **a** successful detonation initiation ( $\Delta t_d = 214 \mu s$ ), and **b** initiation failure ( $\Delta t_d = 211 \mu s$ ) in the setup of Fig. 17. Records PT1, PT2, and PT3 correspond to pressure transducers in Fig. 17. A control channel shows a record of the discharge circuit with two dischargers. Mean detonation velocity in the run with successful detonation initiation is  $1,700 \pm 21$  m/s

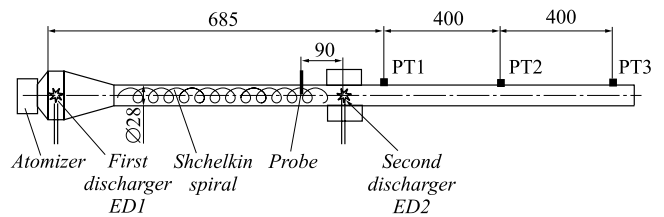


**Fig. 20** Schematic of the detonation tube with the Shchelkin spiral between two dischargers. PT1, PT2, and PT3 denote pressure transducers. Dimensions are in millimeters

Several sets of experiments were made to check the possibility to amplify the primary shock wave exiting from the spiral by the properly tuned triggering of the second discharger. In these experiments, the capacitances of the dischargers, voltage, and the time delay  $\Delta t_d$  of the second discharger triggering relative to the probe activation were varied. When the total initiation energy  $E$  was less than 600 J,

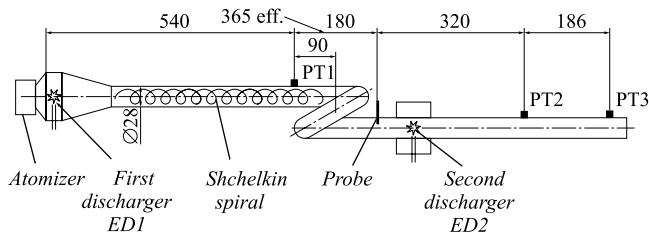


**Fig. 21** Schematic of the detonation tube with the Shchelkin spiral and tube coil between two dischargers. PT1, PT2, and PT3 stand for pressure transducers. Dimensions are in millimeters

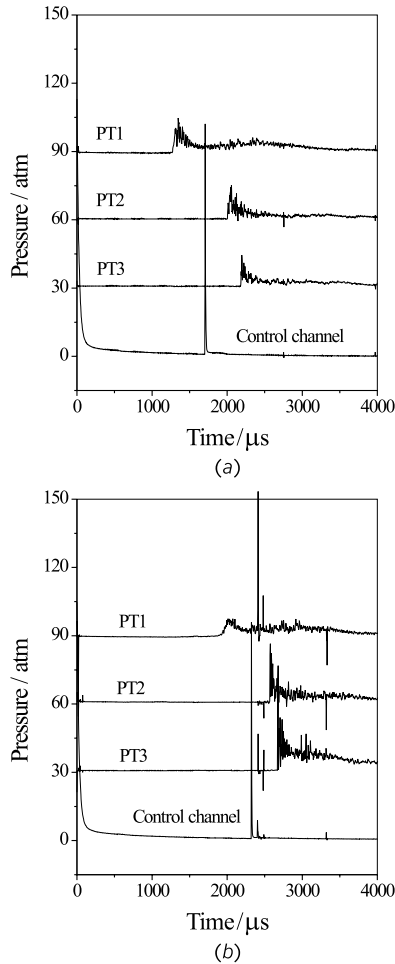


**Fig. 22** Pressure records obtained in the setup of Fig. 21 with triggering only first discharger of 144 J **a** (detonation initiation failed) and two dischargers of total energy 132 J **b** (detonation is successfully initiated)

detonation was not initiated at any  $\Delta t_d$ . When  $E$  was at a level of 650 J, a detonation was initiated at  $\Delta t_d$  varying from 60 to 120  $\mu\text{s}$ . Thus, the detonation peninsula in the tests with the Shchelkin spiral appeared to be considerably wider than in the tests without spiral.

To further decrease the initiation energy of a detonation, the tube was modified as shown in Fig. 21. An additional element, tube coil, was installed after the spiral section. As

the tube coil introduces expansive and compressive surfaces for the propagating shock wave, it was expected that the interactions between various wave systems would promote the detonation onset as shown by Nettleton [2]. In fact, the use of two successively triggered dischargers separated by the Shchelkin spiral and the tube coil resulted in a decrease of the critical detonation initiation energy  $E_{\min}$  in the 28-mm diameter tube to the value of 100 J. In the setup of Fig. 21, the spray detonation is initiated at a distance of about 1 m, that is the predetonation length-to-diameter ratio is about 36.

Figure 22a shows pressure records obtained in the setup of Fig. 21 with triggering only the first discharger of 144 J ( $U = 2,400$  V,  $C_1 = 50 \mu\text{F}$ ) rated energy. At this ignition energy, detonation is not initiated. However, when two dischargers are triggered successively with a total energy of 132 J ( $C_1 = C_2 = 25 \mu\text{F}$ ,  $U = 2,300$  V) and  $\Delta t_d = 80 \mu\text{s}$  (Fig. 22b), a detonation was detected at the tube segment PT2–PT3.

## 5 Discussion

Experimental studies described in Sect. 4 indicate that there exist several principles that allow decreasing the critical energy of spray detonation initiation by electric discharges.

One of the most promising principles is the use of two or more successively triggered dischargers rather than a single discharger [9, 10, 11, 12]. Distributed dischargers artificially induce exothermic reactions in the close vicinity to a relatively weak primary shock wave and stimulate strong coupling between the shock wave and energy deposition leading to the onset of detonation. In experiments reported herein, two dischargers were used. It has been shown that the precise timing of second discharger triggering is required for detonation initiation to minimize the total initiation energy. In these conditions, the energy deposited by each discharger is considerably less than that required for detonation initiation by a single discharger. The use of external energy sources for initiating detonation was first suggested by Zel'dovich and Kompaneetz [13]. Later, this issue was studied computationally by Thibault et al. [14], Yoshikava et al. [15], and Frolov et al. [11] and reviewed elsewhere [3, 16]. For gaseous mixtures (propane–air), detonation initiation by distributed dischargers (up to 7) has been demonstrated experimentally by Frolov et al. [9, 11].

The total detonation initiation energy is very sensitive to the positioning of the dischargers. To generate a stronger primary shock wave at minimal energy requirements, the first discharger must be positioned near the closed end of the detonation tube. The critical initiation energy increases with the distance between the discharger and the tube end. Moreover, there exist an optimal distance between the first and the second dischargers. If the dischargers are located at a short distance  $L$  from each other, they induce a nearly constant-volume explosion of the reactive mixture in volume  $SL$ , where  $S$  is the tube cross-section. This case corresponds to detonation initiation by a single discharge of larger

dimensions. If the dischargers are positioned at a large distance  $L$  from each other, the primary shock wave decays and a detonation is to be initiated by solely a second discharger. At the optimal distance  $L$ , the second discharge triggered in the proper time stimulates chemical energy deposition in the vicinity of the primary shock wave at the stage when the latter has not yet been decayed significantly.

The other important issue is the discharge duration or power. Experiments show that the critical total initiation energy increases with discharge duration. Based on available experimental [17, 18, 19], and computational [20] studies of gaseous detonation initiation, it can be anticipated that this effect vanishes as the discharge duration tends to zero or the discharge power approaches infinity. In the single-discharge experiments reported herein, the decrease in discharge duration from 100 to 50  $\mu\text{s}$  resulted in decreasing the critical initiation energy of spray detonation by a factor of more than 2.

For detonation initiation with two successively triggered dischargers, second discharge duration (at fixed energy) determines the extent of coupling between the energy deposition and the primary shock wave. If second discharge duration is long, only a part of available chemical energy is effectively deposited in the vicinity of the primary shock wave, while the remaining part is deposited far from the wave. In this case, the dynamic interaction between the energy deposition and shock wave occurs via the compression waves catching up with the shock wave. This process is similar to DDT and requires long run-up distances.

If discharge duration is short (comparable with or shorter than a characteristic ignition delay time behind a detonation wave [11]) then the energy deposition is strongly coupled with the primary shock wave and amplification of the latter can be anticipated. In the experiments of Fig. 8 with successful detonation initiation, the second discharger was triggered somewhat prior to the arrival of the primary shock wave to the discharger location. The required advance time for discharge triggering depended on the discharge voltage and varied from 10  $\mu\text{s}$  at 3,000 V to 35  $\mu\text{s}$  at 2,500 V. According to Lee et al. [18], and Knystautas and Lee [19], only energy released till the attainment of the maximum power of an igniter is important in the initiation process. For the critical conditions of Fig. 8, the advance time of 35  $\mu\text{s}$  at  $U = U_{\min} = 2,500$  V correlates with the attainment of the first peak on the discharge current curve of Fig. 1b. Thus, chemical energy deposition stimulated by the second discharge should be synchronized with the arrival of the primary shock wave to the discharger location.

The discharge channel dimension is the other important issue that affects the critical energy of detonation initiation. Insulation of the discharge area avoids electric loss to the grounded metal tube walls. The discharge channel has to occupy the largest possible portion of tube cross-section to ensure efficient utilization of available chemical energy for generating a “planar” shock wave. For example, the use of the sliding discharge of Fig. 14 rather than the arc discharge of Fig. 9 resulted in decreasing the critical initiation energy from 820 to 660 J that is by 20%.

The other approach to diminish the critical initiation energy of spray detonation initiation is to decrease the tube diameter to the value close to the limiting tube diameter. In the reported experiments, the smallest tube diameter that allowed successful detonation initiation in the  $n$ -hexane spray–air mixture was 28 mm. As compared to a larger tube (51 mm), detonation initiation energy was decreased by a factor of 4. However, in the 28-mm tube the arising detonations were marginally stable. As experiments show, to initiate detonation by successive triggering of two dischargers in such a tube, it was necessary to accelerate a primary shock wave to velocities exceeding 1,400 m/s (see Figs. 12 and 13). In the larger tube of 51 mm in diameter, this threshold velocity of shock wave was about 1,200 m/s (see Fig. 5).

The geometry of the detonation tube is another issue affecting the critical initiation energy. It has been demonstrated experimentally that the most preferable tube configuration in terms of the minimal energy requirements for detonation initiation is that with a gradual transition between the volume with electric discharger and the tube, like that shown in Fig. 17. Such a configuration allows cumulating the shock wave prior to its arrival at the position of the second discharger.

To further decrease the initiation energy, a powerful electric discharger utilized for generating a primary shock wave can be replaced by a primary shock wave generator comprising a relatively low-energy (50–60 J) electric discharger, Shchelkin spiral, and tube coil. In the experiments, a second discharger was mounted at the exit of the tube coil and was activated in phase with the primary shock wave arrival at its position. Due to interactions between various wave systems in the tube coil formed at expansive and compressive surfaces, the total critical energy of detonation initiation with two successively triggered dischargers was decreased to about 100 J, i.e., by an order of magnitude as compared with the energy ( $\sim 800$ – $900$  J) required for the direct initiation of the  $n$ -hexane spray detonation in the straight 28-mm diameter smooth-walled tube by a single electric discharger. The other important advantage of the modified configuration of the detonation tube is the relatively low sensitivity of the detonation initiation process to the triggering time delay  $\Delta t_d$  of the second discharger as compared to the configurations without the Shchelkin spiral. This effect can be attributed to the transformation of the pressure profile in the primary shock wave from the ‘triangular’ shape in a smooth-walled tube to a nearly stepwise shape in a tube with the spiral.

---

## 6 Concluding remarks

The results of extensive experimental studies on initiation of a confined  $n$ -hexane spray detonation in air have been reported. It has been found that for direct initiation of spray detonation with minimal energy requirements (1) it is worth to use one discharger located at the closed end of the detonation tube and at least one additional discharger downstream from it to be triggered in-phase with primary shock

wave arrival; (2) discharge area should be properly insulated to avoid electric loss to metal tube walls; (3) discharge duration should be minimized to at least  $50 \mu\text{s}$ ; (4) a discharge channel should preferably occupy a large portion of tube cross-section; (5) the test tube should be preferably of diameter close to the limiting tube diameter; (6) a gradual transition between the volume with electric discharger and the tube should be used; and (7) a powerful electric discharger utilized for generating a primary shock wave can be replaced by a primary shock wave generator comprising a low-energy electric discharger, Shchelkin spiral, and tube coil. With these principles applied, the minimal detonation initiation energy of *n*-hexane spray in air was at the level of 100 J. Detonation was obtained at a distance of about 1 m from the atomizer in a tube 28 mm in diameter. These principles can be used to minimize energy requirements for repeated detonation initiation in a pulse detonation engine.

**Acknowledgements** This work was partly supported by the U.S. Office of Naval Research and Russian Foundation for Basic Research.

## References

- Matsui, H., Lee, J.H.: Influence of electrode geometry and spacing on the critical energy for direct initiation of spherical gaseous detonations. *Combust. Flame* **27**, 217–225 (1976)
- Nettleton, M.A.: *Gaseous Detonations*, pp. 98–106. Chapman and Hall, London, New York (1987)
- Roy, G.D., Frolov, S.M., Borisov, A.A., Netzer, D.W.: Pulse detonation propulsion: challenges, current status, and future perspective. *Prog. Energy Combust. Sci.* **30**(6), 545–672 (2004)
- Benedick, W.B., Tieszen, S.R., Knystautas, R., Lee, J.H.S.: Detonation of unconfined large-scale fuel spray–air clouds. In: Kuhl, A.L., Leyer, J.-C., Borisov, A.A., Sirignano, W.A. (eds.) *Dynamics of Detonations and Explosions: Detonations*, vol. 133, pp. 297–310. *Progress in Astronautics and Aeronautics Series*. AIAA Inc., New York (1991)
- Dabora, E.K.: Lean detonation limit of sensitized kerosene sprays in air. In: Kuhl, A.L., Leyer, J.-C., Borisov, A.A., Sirignano, W.A. (eds.) *Dynamics of Detonations and Explosions: Detonations*, vol. 133, pp. 311–324. *Progress in Astronautics and Aeronautics Series*. AIAA Inc., New York (1991)
- Brophy, C.M., Netzer, D.W., Sinibaldi, J., Jonson, R.: Detonation of JP-10 aerosol for pulse detonation applications. In: Roy, G.D., Frolov, S.M., Netzer, D.W., Borisov, A.A. (eds.) *High-Speed Deflagration and Detonation: Fundamentals and Control*, pp. 207–222. Elex-KM Publishers, Moscow (2001)
- Elkoth, M.M.: Fuel atomization for spray modelling. *Prog. Energy Combust. Sci.* **8**(1), 61–91 (1982)
- Frolov, S.M., Basevich, V.Ya., Belyaev, A.A., Posvyanskii, V.S., Smetanyuk, V.A.: Detailed modeling of drop evaporation and combustion. In: Roy, G.D., Frolov, S.M., Starik, A.M. (eds.) *Combustion and Atmospheric Pollution*, pp. 207–213. Torus Press, Moscow (2003)
- Frolov, S.M., Basevich, V.Ya., Aksenov, V.S.: Detonation initiation by controlled triggering of multiple electric discharges. In: Roy, G.D., Mashayek, F. (eds.) *Proceedings of the 14th ONR Propulsion Meeting*, University of Illinois at Chicago, pp. 202–206. Chicago (2001)
- Frolov, S.M., Basevich, V.Ya., Aksenov, V.S., Polikhov, S.A.: Initiation of spray detonation by successive triggering of electric discharges. In: Roy, G.D., Frolov, S.M., Santoro, R., Tsyganov, S.A. (eds.) *Advances in Confined Detonations*, pp. 150–157. Torus Press, Moscow (2002)
- Frolov, S.M., Basevich, V.Ya., Aksenov, V.S., Polikhov, S.A.: Detonation initiation by controlled triggering of electric discharges. *J. Propul. Power* **19**(4), 573–580 (2003)
- Frolov, S.M., Basevich, V.Ya., Aksenov, V.S., Polikhov, S.A. Initiation of confined spray detonation by electric discharges. In: Roy, G.D., Frolov, S.M., Santoro, R., Tsyganov, S.A. (eds.) *Confined Detonations and Pulse Detonation Engines*, pp. 157–174. Torus Press, Moscow (2003)
- Zel'dovich, Ya.B., Kompaneetz, A.S.: *The Theory of Detonation*, pp. 101–112. Gostekhizdat, Moscow (1955)
- Thibault, P.A., Yoshikawa, N., Lee, J.H.S.: Shock wave amplification through coherent energy release. In: *Proceedings 1978 Fall Technical Meeting of the Eastern Section of the Combustion Institute*, Miami Beach, FL, November 30–December 1 (1978)
- Yoshikawa, N., Thibault, P.A., Lee, J.H.S.: Shock wave amplification in non-uniformly preconditioned gas mixtures. In: *Proceedings 1979 Spring Technical Meeting of the Canadian Section of the Combustion Institute*, Kingston, Ontario, 3–4 May 1979
- Lee, J.H.S., Moen, I.O.: The mechanism of transition from deflagration to detonation in vapor cloud explosions. *Prog. Energy Combust. Sci.* **6**(4), 359–389 (1980)
- Bach, G., Knystautas, R., Lee, J.H.: Initiation criteria for diverging gaseous detonations. In: *Proceedings 13th Symposium (International) on Combustion*, The Combustion Institute, pp. 1097–1110. Pittsburgh, PA (1980)
- Lee, J.H., Knystautas, R., Guirao, C.: Critical power density for direct initiation of unconfined gaseous detonations. In: *Proceedings 15th Symposium (International) on Combustion*, The Combustion Institute, pp. 53–68. Pittsburgh, PA (1974)
- Knystautas, R., Lee, J.H.: On the effective energy for direct initiation of gaseous detonations. *Combust. Flame* **27**(2), 221–228 (1976)
- Levin, V.A., Markov, V.V., Osinkin, S.F.: Modeling of detonation initiation in a gaseous combustible mixture by electric discharge. *Chem. Phys. Rep.* **3**(4), 611–618 (1984)